**Earth System
Dynamics
Discussions**

Effects of land cover change on temperature and rainfall extremes in multi-model ensemble simulations

A. J. Pitman[1], N. de Noblet-Ducoudré[2], F. B. Avila[1], L. V. Alexander[1],
J.-P. Boisier[2], V. Brovkin[3], C. Delire[4], F. Cruz[5], M. G. Donat[6], V. Gayler[3],
B. van den Hurk[7], C. Reick[3], and A. Voldoire[4]

[1]ARC Centre of Excellence for Climate System Science, University of New South Wales, Sydney, Australia
[2]Laboratoire des Sciences du Climat et de l'Environnement, Gif-sur-Yvette, France
[3]Max Planck Institute for Meteorology, Hamburg, Germany
[4]Groupe d'étude de l'Atmosphère Météorologique, Toulouse, France
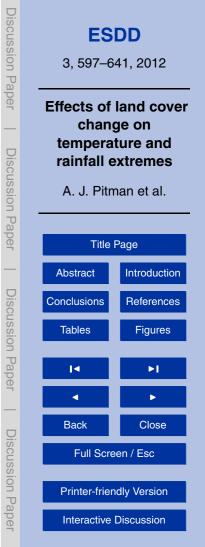[5]Manila Observatory, Quezon City, Philippines
[6]Climate Change Research Centre, University of New South Wales, Sydney, Australia
[7]Royal Netherlands Meteorological Institute, De Bilt, The Netherlands

Correspondence to: A. J. Pitman (a.pitman@unsw.edu.au)

Title Page

Abstract	Introduction
Conclusions	References
Tables	Figures

| ◄◄ | ►► |
| ◄ | ► |

Back | Close

Full Screen / Esc

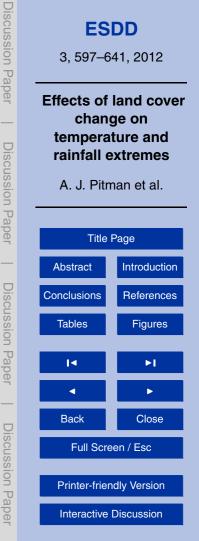Printer-friendly Version

Interactive Discussion

Abstract

The impact of historical land use induced land cover change (LULCC) on regional-scale climate extremes is examined using four climate models within the Land Use and Climate, IDentification of robust impacts project. To assess those impacts, multiple in-
5   dices based on daily maximum and minimum temperatures and daily precipitation were used. We contrast the impact of LULCC on extremes with the impact of an increase in atmospheric CO_2 from 280 ppmv to 375 ppmv. In general, changes in both high and low temperature extremes are similar to the simulated change in mean temperature caused by LULCC and are restricted to regions of intense modification. The impact of
10 LULCC on both means and on most temperature extremes is statistically significant. While the magnitude of the LULCC induced change in the extremes can be of similar magnitude to the response to the change in CO_2, the impacts of LULCC are much more geographically isolated. For most models the impacts of LULCC oppose the im-pact of the increase in CO_2 except for one model where the CO_2-caused changes in
15 the extremes is amplified. While we find some evidence that individual models respond consistently to LULCC in the simulation of changes in rainfall and rainfall extremes, LULCC's role in affecting rainfall is much less clear and less commonly statistically significant, with the exception of a consistent impact over South East Asia. Since the simulated response of mean and extreme temperature to LULCC is relatively large, we
20 conclude that unless this forcing is included we risk erroneous conclusions regarding the drivers of temperature changes over regions of intense LULCC.

1   Introduction

The Land Use and Climate, IDentification of robust impacts (LUCID) project (de Noblet-Ducoudré et al., 2012) is a major international effort to understand the biophysical
25 impacts of land use induced land cover change (LULCC). LUCID used 7 global cli-mate models with prescribed boundary conditions to examine how LULCC affected
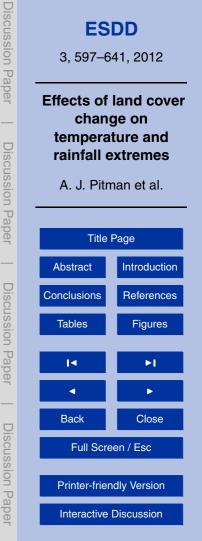
the regional and global mean surface climate. How LULCC affects land-atmosphere interactions is highly complex because a major change to land cover has competing impacts. LULCC, in the form of clearance for crops and pasture, affects net radiation and the partitioning of available energy at the surface. Since conversion of native vege-
tation to crops and pasture typically increases albedo, it reduces net radiation (Forster et al., 2007), which tends to cool the surface. However, changes in leaf area index, aerodynamic roughness length, stomatal conductance and the seasonality of vegetation cover also tend to decrease evapotranspiration and increase sensible heat fluxes (Bala et al., 2007; Pitman et al., 2009). This change in the surface energy balance
can lead to regional scale warming. In the context of LUCID, de Noblet-Ducoudre et al. (2012) and Boisier et al. (2012) provide an in-depth analysis of these issues.

In general, the albedo effect tends to dominate over the mid-latitudes, enhanced by increases in snow-cover, while the role of evapotranspiration and aerodynamic roughness length tends to dominate over the tropics (Davin and De Noblet-Ducoudre, 2010).
Hence, in terms of the averages, the biophysical impact of LULCC is to typically warm the tropics and cool the mid-latitudes (Lawrence and Chase, 2010). This difference in the sign of the impact of regional LULCC results in negligible changes in key climate variables such as temperature and rainfall when averaged globally (Feddema et al., 2005; Pielke et al., 2011). At regional scales, however, in regions subjected to
significant LULCC, the impact of landscape change on temperature and some hydrometeorological variables can be similar in magnitude to a doubling of atmospheric CO_2 (Zhao and Pitman, 2002; Voldoire, 2006) or other large-scale changes in forcing such as the El Niño-Southern Oscillation (Findell et al., 2009). There is also a complex interaction between changes in rainfall, snowfall and/or temperature and the impact of
LULCC, particularly under elevated CO_2 (Pitman et al., 2011). A detailed examination of the observational and model-based evidence linking LULCC to local, regional and global scale climate has recently been provided by Pielke et al. (2011).

While a focus on how LULCC affects global and regional mean surface climate is understandable (at the annual, seasonal and interannual time scales), there is also a

⏮ | ⏭

◀ | ▶

Back | Close

Full Screen / Esc

Printer-friendly Version

Interactive Discussion

A. J. Pitman et al.

Back | Close

Full Screen / Esc
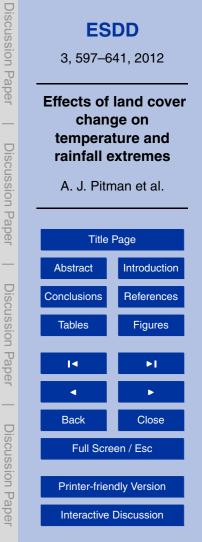
Printer-friendly Version

Interactive Discussion

need to examine how climate extremes are affected by landscape change. Observations demonstrate that extremes are changing (IPCC, 2012). Since the middle of the 20th century there has been a positive (warming) shift in the distribution of daily minimum temperature throughout the globe (Caesar et al., 2006), manifested by a significant increase in the number of warm nights globally (Alexander et al., 2006). A positive shift in the distribution of daily maximum temperature has also been observed, although somewhat smaller than the increase in daily minimum temperature. There have also been statistically significant trends in the number of heavy precipitation events in some regions (IPCC, 2012).

LULCC also affects extremes (Pielke et al., 2011). The nature of the land surface affects the capacity to supply water to be evaporated at the surface and this can amplify or suppress meteorologically driven extremes. For example, Teuling et al. (2010) highlighted how forest and grassland regions of Europe responded to heatwaves, identifying a stronger drought control by forests compared to grassland. Stefanon et al. (submitted) demonstrated considerable sensitivity in these phenomenon associated with how vegetation phenology is represented. Once linked with the impact of LULCC on land-atmosphere coupling (Seneviratne et al., 2006, 2010) and the recognition that the surface energy balance is strongly affected by the nature of the land cover (Pitman, 2003; Bonan, 2008; Levis, 2010; Boisier et al., 2012) it is plausible that LULCC could affect temperature extremes provided it is of a sufficient scale and intensity.

There is also a potential link between LULCC and rainfall extremes (Pielke et al., 2011) either directly via a change in the land forcing on the boundary layer (Pielke, 2001; Niyogi et al., 2011) or via impacts on horizontal temperature gradients and advection of heat and moisture (Gero and Pitman, 2006; Chang et al., 2009).

To explore the impacts of LULCC on extremes, Avila et al. (2012) used a coarse resolution global climate model and examined the simulated daily maximum and minimum temperature. They followed the recommended methods from the joint Commission for Climatology (CCL), the Climate Variability and Predictability (CLIVAR) Programme of the World Climate Research Programme (WCRP) and the Joint World Meteorological
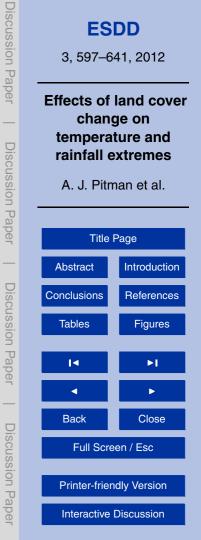
Organization-Intergovernmental Oceanographic Commission Technical Commission for Oceanography and Marine Meteorology (JCOMM) Expert Team on Climate Change Detection and Indices (ETCCDI) (Alexander et al., 2006). Due to the coarse resolution of the model, they did not examine changes in precipitation. This paper extends the study by Avila et al. (2012) in two ways. First, we report on the impact of LULCC over four different global climate models to produce a more reliable estimate than Avila et al. (2012). Second, we use climate models with a finer spatial resolution. We therefore also include the impact of LULCC on rainfall extremes, although we are cautious in our interpretation of these results given the challenge of simulating accurate rainfall statistics in global climate models.

2 Methodology

2.1 Experimental design

Four climate models coupled to different land surface models were used (Table 1). These are a sub-set of the models reported by de Noblet-Ducoudre et al. (2012) because the calculation of the ETCCDI indices requires daily data and only these four modelling groups saved daily temperature and rainfall data. Details of the models used, the land surface schemes and how LULCC was implemented in each modelling system is provided by de Noblet-Ducoudré et al. (2012). We omit results from Avila et al. (2012) because they did not use the LUCID experimental design.

All models undertook simulations representing present day and pre-industrial greenhouse gas concentrations and sea surface temperatures (SSTs) (Table 2). Both SSTs and sea ice extent were prescribed to vary interannually and seasonally using the Climate of the 20th Century project specifications (see HadISST1.1, ftp://www.iges.org/pub/kinter/c20c/HadISST/). Each model undertook simulations forced with two different vegetation distributions (representative of 1870 or 1992) and carried out at least 5 independent simulations for each experiment to help determine those changes that were
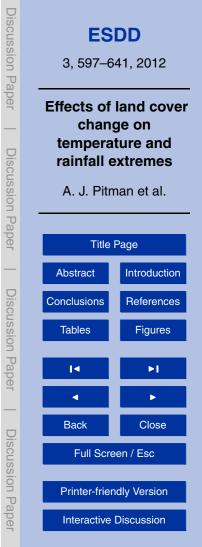
robust from those that reflected internal model variability. The independent simulations were combined (not averaged) before calculating the indices. Hence, each member of an ensemble is accounted for in calculation of the indices and in the calculation of the statistical significance of changes in the extreme indexes.

For the vegetation distribution, each model was provided the same distribution of crop and pasture at a resolution of $0.5° \times 0.5°$ obtained from respectively Ramankutty and Foley (1999) for crops and Goldewijk (2001) for pasture, and each group imposed this crops and pasture distribution onto their existing vegetation map. Natural vegetation for each map, and therefore each group, at each time period (1870 or 1992) therefore either comes from a potential vegetation map, or from an enlargement/contraction of present-day natural vegetation, while the extent of crops and pasture comes from the datasets provided. Note that the scale of croplands is geographically quite extensive but the intensity of croplands only exceeds 50 % over large areas in eastern United States, Western Europe and parts of South East Asia. However, the intensity of LULCC varies between the four climate models (Fig. 1) despite the use of the same input data sets because each modelling group implemented the area of cropland and pasture independently (see de Noblet-Ducoudré et al., 2012).

Our experiments are conducted as follows. We represent the change due to CO_2 via the difference between simulations using near present day CO_2 (375 ppm) with land-use representing 1870 (experiment PDv) differenced from simulations using an identical configuration except CO_2 was set to 280 ppm (experiment PI). Thus PDv-PI, which both use 1870 land-use, captures the impact of a change in CO_2. A second set of results examines the impact of LULCC. To examine the impact of LULCC at 280 ppm, experiments are undertaken with 1992 land-use (experiment PIv) and 1870 land-use (experiment PI) and are represented by the difference PIv-PI. A parallel experiment at 375 ppm is also conducted with land-use representing 1992 (experiment PD) and 1870 (experiment PDv) represented by the difference PD-PDv. Details on the experiment configuration are provided in Table 2.
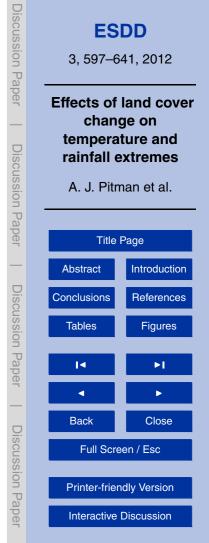
2.2 Extreme indices

We used the ETCCDI indices in this paper. They are calculated from daily maximum and minimum temperature and daily precipitation, and have been developed to assess changes in intensity, duration and frequency of extreme climate events. While the ETCCDI indices do not always represent the largest extremes, they provide globally coherent measures of more moderate extremes that can be useful for global climate change impact assessments (Klein Tank and Zwiers, 2009; Zhang et al., 2011). Details of the indices used in this study are provided in Table 3.

To derive the indices, the simulation PI was used as the reference distribution. For each model and each experiment, all 5 runs were concatenated (combined into a single data set) before the indices were calculated. For indices based on percentiles (TN10p, TX10p, TN90p, TX90p, CSDI, WSDI), the daily 10th and 90th percentiles from the PI simulation are also used as thresholds when calculating the indices for the other simulations (i.e. Plv, PD, PDv). To aid comparison between the models, the daily temperature and precipitation data were interpolated to a common grid before calculating the indices.

2.3 Assessing local significance

Since the distribution of the indices is not necessarily Gaussian, a parametric test such as Student's t-test may be inappropriate for testing the null hypothesis that there is no statistically significant difference between the simulations for a given index. We therefore use the two-tailed Kolmogorov-Smirnov test, which is a non-parametric test that makes no assumptions about the distribution of the data. This method was used by Deo et al. (2009) and Avila et al. (2012) in studies of climate extreme indices. Grid points with statistically significant differences are shown in colour in the bubble maps with red indicating warmer and drier and blue indicating cooler and wetter climates. For each of the regions of interest (Northern Hemisphere, 0–70° N, 180° W–180° E; North
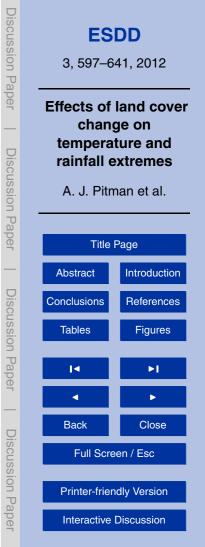
3 Results

3.1 Mean impact of LULCC at different levels of atmospheric carbon dioxide

We begin with a brief discussion of how LULCC and the change in CO_2 affect the mean temperature and rainfall because these changes help explain how extremes change. Figure 2 shows the impact of LULCC on the mean temperature in March-April-May (MAM) and June-July-August (JJA) at 280 ppmv and 375 ppmv. To act as a reference to the impact of LULCC, the response to solely an increase in CO_2 on temperature is also shown. In terms of the mean response, in MAM and JJA, LULCC tends to cool the northern hemisphere mid-latitudes but the response is varied ranging from a strong response in ARPEGE and ECEarth to a weaker response in ECHAM5 and a warming in IPSL in JJA. The explanation for these different responses in the mean temperature was provided by de Noblet-Ducoudré et al. (2012) and is related to both the intensity of land cover change (note, Fig. 1 shows ECHAM5 to implement change somewhat less intensely that ARPEGE or ECEarth), and how crops are parameterized in the model. There are three conclusions from Fig. 2. First, the impact of LULCC is broadly similar at both 280 ppmv and 375 ppmv and in both cases LULCC causes mid-latitude cooling (except for the warming in IPSL during JJA), reaching 2 °C in some regions. Second, the increase in CO_2 from 280 ppmv to 375 ppmv causes large-scale warming of mainly 0.4–1.5°C. Third, the increase in CO_2 leads to warming almost everywhere while LULCC tends to have a more regionalized impact. An interesting result in JJA is that the model with the largest global warming due to the increase in CO_2 (ECHAM5) is the model with the weakest sensitivity to LULCC. While this suggests that a model's sensitivity to a land cover perturbation is not directly proportional to the
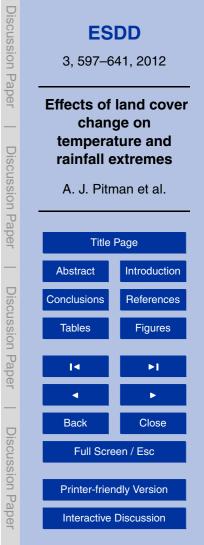
model sensitivity to the CO_2 forcing, this is complicated by the intensity of LULCC, which varies between the models.

In terms of precipitation, Fig. 3 shows the mean model response to LULCC and to the increase in CO_2 from 280 ppmv to 375 ppmv. The impact of LULCC on precipitation is generally weak in all models at both 280 ppmv and 375 ppmv. However, there are similarities between the impacts of LULCC at the two CO_2 levels particularly in JJA. At both 280 ppmv and 375 ppmv, ARPEGE simulates a small increase of summer precipitation over Eurasia and a decrease over North America; ECHAM5 simulates a small increase over parts of North America; ECEarth simulates increase over North America and Eurasia and IPSL simulates decreases over North America and Eurasia. If LULCC did not affect rainfall, then the individual regions affected by rainfall changes in Fig. 3 would likely vary randomly between the results at 280 ppmv and 375 ppmv. Since there are similarities in the regional pattern of change in rainfall due to LULCC at both CO_2 levels it is likely that while the models disagree on the sign of the impact of LULCC on precipitation, internally each model is affected by LULCC in a consistent way.

The apparent decreases in rainfall over S. E. Asia simulated by all models in JJA due to LULCC at both 280 ppmv and 375 ppmv are intriguing (Fig. 3). The response is weaker in ARPEGE and ECHAM5 which is expected because the models also simulate a weaker response to LULCC elsewhere (in part due to a smaller intensity of LULCC in ECHAM5, see Fig. 1). The decline in mean rainfall covers a large region of S. E. Asia, particularly in ECEarth and IPSL, and occurs at both 280 and 375 ppmv. Similarly, the increases in precipitation over S. E. Asia in both MAM and JJA due to the increase in CO_2 and associated changes in sea surface temperatures are also consistent between the models. In general, the pattern of the CO_2-induced precipitation changes agree much better between the models than for LULCC-induced changes, pointing at more complex processes and feedbacks linking how the land-surface is parameterized and rainfall, than between changes in GHG concentrations and rainfall.
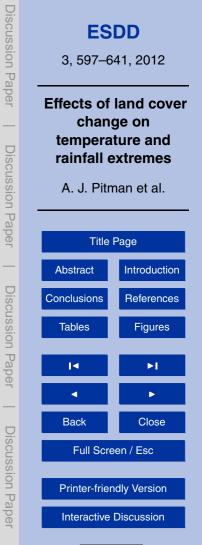
Overall, LULCC over S. E. Asia appears to decrease rainfall in all models, which is the opposite signal due to the increase in CO_2, which leads to increased precipitation in all models. Our results suggest that simulations of the impact of increasing CO_2 over S. E. Asia that omit the impacts of LULCC will lead to erroneous conclusions on the precipitation response when discussing anthropogenic induced climate change. However, the magnitude of the impact of LULCC on rainfall ($\pm 1\,\mathrm{mm\,day^{-1}}$) is not particularly large and the CO_2 change included here is not representative of mid- to late-21st century levels. While LULCC may well continue to be intensive in S. E. Asia, increases in CO_2 will likely remain the dominant regional forcing on rainfall throughout the 21st century.

3.2 Impact of LULCC on temperature intensity extremes

The impact of LULCC on TXx (warmest seasonal daily maximum temperature) is shown in Fig. 4 for MAM and JJA. In MAM, a reduction in TXx is simulated due to LULCC by models over some parts of North America but the scale of the reduction varies in spatial scale from most of North America (ECEarth) to just a few grid points (ECHAM5). ECHAM5 simulates a region of increase in TXx coincident with the most northern region of LULCC (Fig. 1) over North America. Results are generally consistent over North America between the models at both 280 ppmv and 375 ppmv. Over Eurasia, ECEarth simulates a larger region of decreases in TXx in comparison to the other models and ECHAM5 simulates increases in TXx at 375 ppmv. The impact of the increase in CO_2 on TXx is generally more widespread and is almost always an increase. Thus, in most models the CO_2 induced increase in TXx is suppressed by LULCC. In the case of ECEarth and IPSL, the decrease in TXx due to LULCC in MAM would dominate the change due to an increase in CO_2 reversing the sign of the change over Eurasia and over large parts of North America. Results are similar for JJA with the exception of IPSL, which simulates an increase in TXx, amplifying the impact of increased CO_2 while the other models simulate a decrease in TXx locally suppressing the response to CO_2. The increase in IPSL is associated with the mean temperature

change (Fig. 2). In both MAM and JJA, the scale of impact of LULCC on TXx is of a similar magnitude, but much less widespread, than the impact of increasing CO_2. Note that there are no changes in TXx remote from regions of LULCC that are consistent between the models.

⁵   Comparing Fig. 2 with Fig. 4 suggests some relationship between the change in the mean surface air temperature and the change in TXx for LULCC in both MAM and JJA. However, while the sign of the change in TXx accurately reflects the sign of the change in the mean, and to some degree the magnitude of the change in the mean is proportional to the change in the magnitude of TXx, this is model dependent. The

¹⁰ relationship between the change in the mean and the change in TXx is relatively strong in ECEarth for all regions of significant LULCC. In contrast, the relationship is weaker for ARPEGE but there is still a tendency for a large increase in the mean to be reflected by a larger increase in TXx. There is little relationship between the change in the mean and the change in TXx in ECHAM5 and IPSL. Boisier et al. (2012) explored the role

¹⁵ of the total turbulent energy flux (the sum of the sensible and latent heat fluxes) in explaining the impact of LULCC. We also explored whether the change in the total turbulent energy flux could be correlated with the change in TXx but could find no relationship.

A similar pattern of results is shown in Fig. 5 for TNn (coldest seasonal daily minimum

²⁰ temperature). LULCC reduces TNn in MAM and in JJA by similar amounts at 280 ppmv and 375 ppmv and in both cases this offsets increases in TNn due to the increase in CO_2. In MAM and JJA there is quite a large response in TNn to LULCC in ARPEGE and ECEarth and a weak response in ECHAM5 and IPSL. The relationship between the change in the mean temperature and TNn is very similar to that discussed for TXx.

²⁵ As with TXx, there are no changes in TNn remote from regions of LULCC that are consistent between the models.
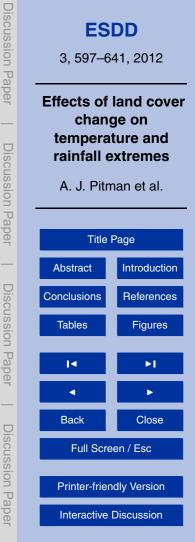
3.3 Impact of LULCC on temperature frequency extremes

The impact of LULCC on TX90p (warm days, defined as the number of days when $T_{max} >$ 90th percentile) shows decreases in this measure over North America and Eurasia in MAM in ARPEGE, ECEarth and IPSL but little change in ECHAM5 (Fig. 6). To allow a comparison of the different forcing effects, all percentile exceedances in Fig. 6 relate to the 10th/90th percentile of daily T_{max} calculated for the PI simulation. There are strong overall similarities between the impact at 280 ppmv and 375 ppmv. As with TXx and TNn, LULCC tends to locally offset the impact of increasing CO_2. Again, in common with the changes in the mean and TXx, IPSL simulates an increase over parts of Europe in JJA in contrast to the decrease simulated by the other models. Thus, in JJA, LULCC locally offsets the impact of increased CO_2 on TX90p in ARPEGE, ECHAM5 and ECEarth but amplifies it in IPSL. Consistent with earlier results there are no changes in TX90p remote from regions of LULCC that are consistent between the models.

Results are very similar for TX10p (cool days, defined as the number of days per season when $T_{max} <$ 10th percentile from the PI simulation, for TN10p (cool nights, defined as the number of days per season when $T_{min} <$ 10th percentile from the PI simulation) and for TN90p (warm nights, defined as the number of days per season when $T_{min} >$ 90th percentile). In each case, the overall impact of LULCC is a cooling (increased TN10p and TX10p, decreased TN90p) of these measures in both North America and Eurasia offsetting the CO_2-induced warming. In each case, IPSL is an exception in JJA where LULCC suppresses the CO_2-induced decreases (TN10p, TX10p) and increases (TN90p) respectively. In all cases, there are no changes remote from regions of LULCC that are consistent between the models.

3.4 Impact of LULCC on temperature duration extremes

The impact of LULCC on WSDI (warm spell duration) is shown in Fig. 7. ARPEGE simulates a decrease in WSDI over Eurasia, IPSL simulates an increase, ECHAM5

and ECEarth simulate negligible change at 280 ppmv. There is a strong amplification of the impact of LULCC at 375 ppmv in ARPEGE over Eurasia and in ECEarth over North America. Both of these amplifications would largely offset the CO_2-induced changes.
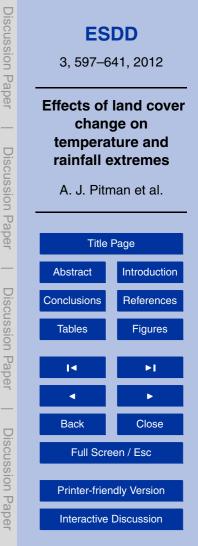
There is a very strong response to LULCC in the cold spell duration (CSDI, Fig. 8) in ARPEGE and ECEarth. Both models simulate a large increase in days with at least 6 consecutive days when $T_{min} <$ 10th percentile at both 280 and 375 ppmv. These changes are large relative to the impact of the increased CO_2 and oppose the sign of the net impact from CO_2 alone. CSDI in ECHAM5 is consistently insensitive to LULCC, which may in part be due to the lower intensity of the LULCC (Fig. 1) although the relationship between the scale of LULCC and its impact on indices such as CSDI are unknown. Changes in CDSI are CO_2 concentration specific and the impact of LULCC declines under higher CO_2 in most models. This decrease is most clear in ECEarth but is also apparent in ARPEGE (North America and S. E. Asia), IPSL (a lot of significant points disappear under higher CO_2). This is likely due to CO_2-induced warming and a loss of snow cover that reduces the sensitivity of the climate to LULCC (Pitman et al., 2011). Again, consistent with earlier results there are no changes in either CSDI or WSDI remote from regions of LULCC that are consistent between the models.

3.5 Impact of LULCC on rainfall extremes

We include results from the four models for one rainfall index (RX5day, the maximum rainfall occurring over a 5-day period). Results from RX1day, the maximum rainfall occurring over a 1-day period were similar in geographic extent and of order 20 % of the magnitude shown for RX5day.

The impact of LULCC on RX5day is highly variable. Figure 9 shows both increases and decreases in RX5day for MAM and JJA. There is a co-location of decreases in RX5day and LULCC over North America and Eurasia in both seasons in ARPEGE at 280 ppmv, but not at 375 ppmv. RX5day increases and decreases over North America in JJA in ECHAM5 at both CO_2 levels. There are increases in RX5day at 375 ppmv in

JJA in ECEarth, but not at 280 ppmv. Finally, RX5day is reduced in IPSL at both levels of CO_2 in JJA.

One would expect the largest impact of LULCC on rainfall extremes to be during summer coincident with high net radiation, surface evaporation and convection. The JJA results from ARPEGE and IPSL suggest that rainfall extremes in these models do respond to LULCC and both models show a decrease of extreme precipitation at many grid boxes affected by LULCC. However, even in JJA there are major inconsistencies in how ARPEGE and IPSL respond to LULCC at the two CO_2 levels. Further, ECHAM5 and ECEarth do not hint at a large change in RX5day. It is therefore very difficult to conclude anything in terms of extreme rainfall from our results.

We explored the relationship between changes in RX5day and mean rainfall, and between RX5day and the total turbulent energy flux (Q_t) for each model (Table 4). We found a reasonably strong and consistent relationship between changes in mean rainfall and changes in RX5day in ECEarth in all three regions of LULCC. This relationship was weaker for ARPEGE and non-existent for IPSL and ECHAM5. A similar result is shown in Table 4 for the relationship between RX5day a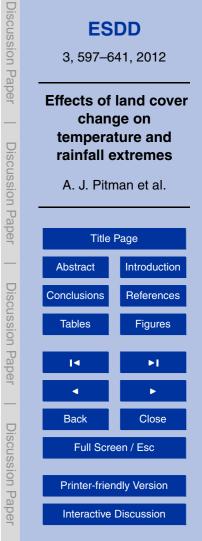nd the total turbulent energy flux. ECEarth and to a weaker degree ARPEGE show a correlation between these quantities, but there is none for IPSL or ECHAM5.

Finally, the scale of the simulated change in RX5day is worthy of note. The largest change in RX5day is of order $2\,\mathrm{mm\,day^{-1}}$ in the 5-day rainfall total on the seasonal timescale (Fig. 9). In the four models used here, even if LULCC does perturb rainfall extremes, the scale of the change is very small relative to the size of the event.
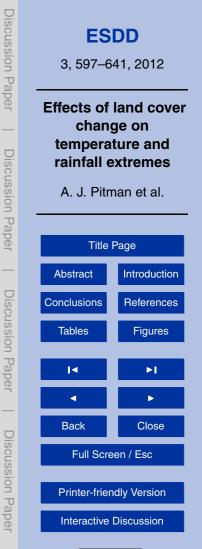
4 Discussion

There is a strong consensus that LULCC affects the mean climate of regions that have been transformed by human activity (Pielke et al., 2011). In common with some other processes, such as cloud cover induced feedbacks on the surface radiation balance (van der Molen et al., 2011), LULCC appears to have a clear zonal signature. This

paper examines how LULCC affects four climate models' simulation of temperature and rainfall extremes using a selection of the ETCCDI extreme climate indices. This work builds on earlier analyses of how LULCC affects the mean climate (de Noblet-Ducoudré et al., 2012; Boisier et al., 2012).

Several of our results reflect earlier studies well. Our results suggest broadly similar impacts from LULCC in the temperature and rainfall indices at 280 and 375 ppmv. This increase in CO_2 is not representative of future simulations where concentrations might double or triple so we cannot infer the impact of LULCC on the ETCCDI indices in future climate projections. However, at the levels of CO_2 reached to date, the regional impact of LULCC on temperature and rainfall appear similar in magnitude to the CO_2 effect in regions of intense LULCC. This is useful because the forced change in CO_2 and associated SSTs leads effectively to a new simulation by each model. The recognition that the impact of LULCC is similar across these various simulations of a given model helps reinforce the robustness of the impact of LULCC shown here. Our results also agree with earlier studies that the impact of LULCC on the mean temperature and rainfall is generally coincident with regions of intense land cover change. We extend this result to the ETCCDI extreme indices. Since the impacts of LULCC are largely isolated to the regions of intense land cover change, they are geographically isolated in comparison to the impact of increased CO_2. This conclusion does not preclude the existence of remote changes due to LULCC, in particular because we used fixed sea surface temperatures, but in the models explored here there are no changes simulated remote from LULCC that are common to all four models in either the mean or extremes.

In terms of the impact of LULCC on the ETCCDI indices, the cooling in mean temperature due to LULCC, particularly in the mid-latitudes (Fig. 2), is related to reductions in most of the temperature indices including TXx, TNn, and TX90p. The increase in JJA temperatures due to LULCC in IPSL is also related to increases in TXx, TNn, and TX90p. There is not, however, a simple relationship between these extremes indices and the mean change in all models. While the sign of the change in the mean temperature accurately predicts the sign of the change in each extreme in all four models, it is
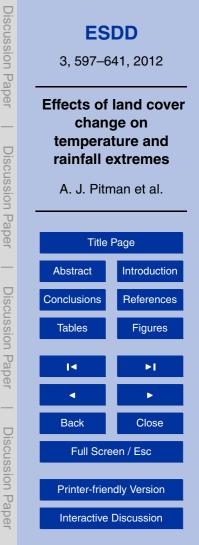
only ECEarth where the magnitude of the change in the mean predicts the magnitude of the change in TXx (and other indices). In terms of rainfall, there is little correlation between the change in mean rainfall and RX5day, apart from a weak correlation in ECEarth. However, in contrast to earlier LUCID results (Pitman et al., 2009) there are suggestive changes in rainfall resulting from LULCC. This was shown, in particular, for S. E. Asia but there are some consistent impacts from LULCC in other regions.

To explore the impact of LULCC at 280 ppmv and 375 ppmv relative to the increase in CO_2 the field significance (see Sect. 2.3) of the changes in each index was derived. The results, shown in Table 5, are expressed as a percentage of grid points that underwent statistically significant changes. The increase in CO_2 from 280 ppmv to 375 ppmv led to statistically significant changes in all temperature indices in all models in both MAM and JJA (Table 5). The number of statistically significant points varied by region, by model, and by season but there is clearly a strong and coherent change in the ETCCDI temperature indices due to the increase in CO_2. In contrast, the rainfall indices change in a smaller percentage of grid points such that in ECEarth and ECHAM5 no statistically significant changes in the rainfall indices occur due to the increase in CO_2 in some regions. In terms of LULCC's impact on the ETCCDI indices, the percentage of points showing a field significant change is smaller than the impact due to increased CO_2, but the impact of LULCC is not negligible. One would expect a smaller impact because while increased CO_2 affects every grid point within every region, there are grid points within each region where there is no, or only a very weak land cover perturbation. Despite this contrast between the scale of perturbation, in ARPEGE, ECEarth and to a smaller degree IPSL, 20–40 % of grid points undergo statistically significant changes in the temperature indices in both MAM and JJA following LULCC. ECHAM5, which demonstrated a relatively high sensitivity to the change in CO_2, is the least sensitive to LULCC with only the eastern region of the US experiencing more than 40 % of grid points undergoing field significant change. However, this is likely related, at least in part, to the relatively low intensity of LULCC imposed in the model (Fig. 1). While the percentage of grid points undergoing significant change in the rainfall indices due to
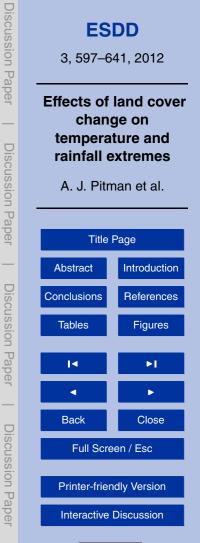
LULCC is generally small, in JJA the scale of impact is not much smaller than the impact due to the increase in CO_2.

Our results have interesting implications for those analysing the impact of anthropogenic climate change on the ETCCDI indices from climate model simulations that did not include LULCC. As shown by Avila et al. (2012) in the case of some indices, where LULCC triggers regional-scale changes of similar scale to the imposed increase in CO_2, interpretation of climate model results should be undertaken very cautiously. Most commonly, in regions of intense LULCC, land cover change would offset the impact of elevated CO_2. Surprisingly, this also included partially offsetting a CO_2 induced increase in rainfall over S. E. Asia in three of the four models. In some regions, LULCC perturbs the ETCCDI indices to amplify the impact of elevated CO_2 (e.g. IPSL for TXx over Eurasia). Clearly, changes in ETCCDI temperature indices cannot be approximated by just changing CO_2 in regions of intense LULCC. More seriously, if a model does capture the observed changes in TXx or other indices *without* representing LULCC, our results suggest a significant risk that the model would be obtaining the right answers for the wrong reasons.

Finally, we note that in terms of changes in ETCCDI rainfall indices we restricted our analysis to RX5day but noted that RX1day showed a similar behaviour with respect of both changes in CO_2 and LULCC. Our results cannot confirm or deny a role of large-scale LULCC on rainfall extremes. The results from the four models are too inconsistent to permit a clear relationship to be identified. While an individual model tended to respond to LULCC in terms of mean rainfall consistently at the two levels of CO_2. However, there was no consistency between the four models in the direction or magnitude of change in RX5day due to LULCC (Fig. 9). It is likely that the four models we analyse here remain too coarse in terms of spatial resolution or the simulations remain too short to identify a signal, or it may be that LULCC experienced to date does not affect regional-scale rainfall or rainfall extremes.
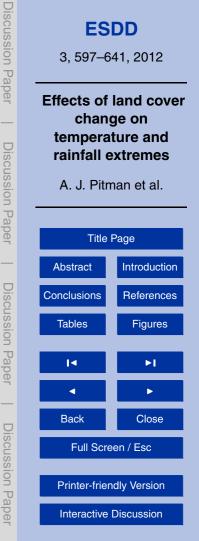
5   Conclusions

The impact of LULCC on regional-scale climate averages has been thoroughly studied and a significant impact on the mean temperature should be anticipated over regions of intense LULCC (Pielke et al., 2011). However, the impact of LULCC on climate model simulated extremes has been less well studied. In this paper we used indices recommended by the CCl/CLIVAR/JCOMM Expert Team on Climate Change Detection and Indices (ETCCDI) based on daily maximum and minimum temperature and daily precipitation. Our experimental design used the Land Use and Climate, IDentification of robust impacts (LUCID) project protocol (Pitman et al., 2009; de Noblet-Ducoudré et al., 2012). We investigated the impact of LULCC on selected ETCCDI indices, using four climate models, contrasting the large-scale impact from LULCC with an increase of atmospheric CO_2 from 280 ppmv to 375 ppmv. Our LULCC perturbation focused on conversion of forests to crops and pasture and ignores other types of land use change such as urbanization and irrigation that could also strongly affect regional climate (Pielke et al., 2011) but tend to be more localized. The CO_2 increase and LULCC together reflect significant causes of anthropogenic climate change since the pre-industrial era until today.

Our results demonstrate that the impact of the increase in CO_2 on the ETCCDI indices is much more geographically extensive but often of a similar magnitude than the impact of LULCC. However, many of the temperature indices show locally strong and statistically significant responses to LULCC, such that commonly 30–50 % of the continental surfaces of the tropics and Northern and Southern Hemispheres are affected statistically significantly by LULCC. To avoid any risk of misunderstanding, we remind readers that the increase in CO_2 imposed here is 280 ppmv to 375 ppmv and not an increase representative of future concentrations. We do not imply that LULCC would likely affect the ETCCDI indices as much as a doubling or tripling of CO_2.

There is a great deal more to be done in associating LULCC with temperature and rainfall extremes. LUCID provided a starting point for this analysis but only four models
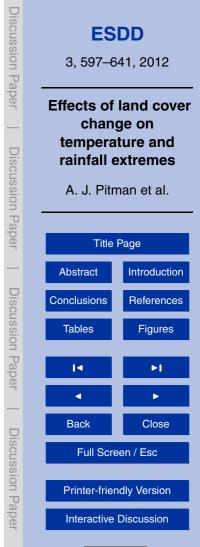
were available, and these four models contrasted sharply in how they responded to LULCC in terms of simulated extremes. De Noblet-Ducoudré et al. (2012) argued that land surface modellers should evaluate models using observations where land use change has been imposed in order to better resolve how this change affects the mean climate. Analyses of these types will also help resolve the impact of LULCC on extremes.

We conclude that in terms of using the ETCCDI indices for climate impacts studies at large spatial scales, LULCC needs to be incorporated only where LULCC has been intensive. These regions of intensive LULCC are, of course, closely correlated with human population density. In some cases, LULCC affects the ETCCDI indices in the same direction as increasing CO_2, in other cases LULCC masks changes due to increasing CO_2. In general, these compensation/amplification phenomenon complicate the use of ETCCDI indices in regional detection and attribution studies. However, they also provides a useful future path for detection and attribution studies since if LULCC is explicitly included, a clearer signal should be possible, providing an improved capacity to attribute observed and modelled trends to known forcings.

References

Alexander, L. V., Zhang, X., Peterson, T. C., Caesar, J., Gleason, B., Klein Tank, A. M. G., Hay-lock, M., Collins, D., Trewin, B., Rahimzadeh, F., Tagipour, A., Rupa Kumar, K., Revadekar, J., Griffiths, G., Vincent, L., Stephenson, D. B., Burn, J., Aguilar, E., Brunet, M., Taylor, M., New, M., Zhai, P., Rusticucci, M., and Vazquez-Aguirre, J. L.: Global observed changes in daily climate extremes of temperature and precipitation, J. Geophys. Res., 111, D05109, doi:10.1029/2005jd006290, 2006.

Avila, F. B., Pitman, A. J., Donat, M. G., Alexander, L. V., and Abramowitz, G.: Climate model simulated changes in temperature extremes due to land cover change, J. Geophys. Res., 117, D04108, doi:10.1029/2011jd016382, 2012.

Bala, G., Caldeira, K., Wickett, M., Phillips, T. J., Lobell, D. B., Delire, C., and Mirin, A.: Com-bined climate and carbon-cycle effects of large-scale deforestation, P. Natl. Acad. Sci., 104, 6550–6555, doi:10.1073/pnas.0608998104, 2007.

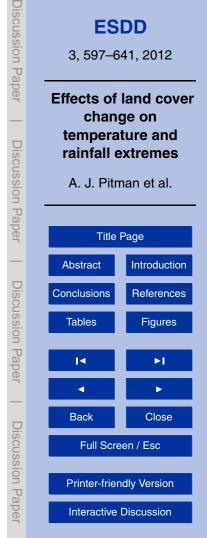Boisier, J.-P., de Noblet-Ducoudré, N., Pitman, A. J., Cruz, F., Delire, C., van den Hurk, B. J. J. M., van der Molen, M. K., Müller, C., and Voldoire, A.: Attributing the biogeo-physical impacts of land-Use induced land-cover changes on surface climate to specific causes. Results from the first LUCID set of simulations, J. Geophys. Res., 117, D12116, doi:10.1029/2011JD017106, 2012.

Bonan, G. B.: Forests and Climate Change: Forcings, Feedbacks, and the Climate Benefits of Forests, Science, 320, 1444–1449, doi:10.1126/science.1155121, 2008.

Caesar, J., Alexander, L., and Vose, R.: Large-scale changes in observed daily maximum and minimum temperatures: Creation and analysis of a new gridded data set, J. Geophys. Res., 111, D05101, doi:10.1029/2005jd006280, 2006.

Chang, H.-I., Niyogi, D., Kumar, A., Kishtawal, C. M., Dudhia, J., Chen, F., Mohanty, U. C., and Shepherd, M.: Possible relation between land surface feedback and the post-landfall struc-ture of monsoon depressions, Geophys. Res. Lett., 36, L15826, doi:10.1029/2009gl037781, 2009.

Davin, E. L. and De Noblet-Ducoudre, N.: Climatic Impact of Global-Scale Deforestation: Ra-diative versus Nonradiative Processes, J. Climate, 23, 97–112, 2010.

de Noblet-Ducoudré, N., Boisier, J.-P., Pitman, A., Bonan, G. B., Brovkin, V., Cruz, F., Delire, C., Gayler, V., van den Hurk, B. J. J. M., Lawrence, P. J., van der Molen, M. K., Müller, C., Reick, C. H., Strengers, B .J., and Voldoire, A.: Determining robust impacts of land-use induced
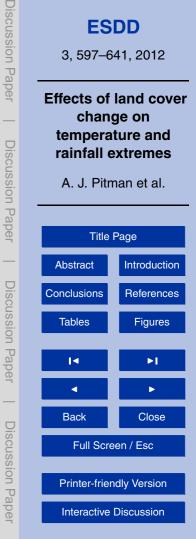
land-cover changes on surface climate over North America and Eurasia; Results from the first set of LUCID experiments, J. Climate, 25, 3261–3281, doi:10.1175/jcli-d-11-00338.1, 2012.

Deo, R. C., Syktus, J. I., McAlpine, C. A., Lawrence, P. J., McGowan, H. A., and Phinn, S. R.: Impact of historical land cover change on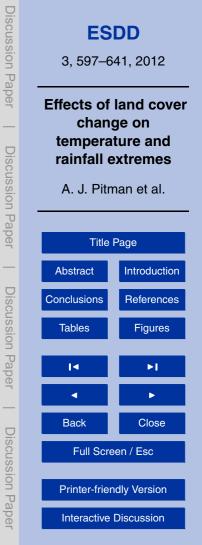 daily indices of climate extremes including droughts in eastern Australia, Geophys. Res. Lett., 36, L08705, doi:10.1029/2009GL037666, 2009.

Feddema, J. J., Oleson, K. W., Bonan, G. B., Mearns, L. O., Buja, L. E., Meehl, G. A., and Washington, W. M.: The Importance of land-cover change in simulating future climates, Science, 310, 1674–1678, doi:10.1126/science.1118160, 2005.

Findell, K. L., Pitman, A. J., England, M. H., and Pegion, P. J.: Regional and Global Impacts of Land Cover Change and Sea Surface Temperature Anomalies, J. Climate, 22, 3248–3269, 2009.

Forster, P., Ramaswamy, V., Artaxo, P., Berntsen, T., Betts, R., Fahey, D. W., Haywood, J., Lean, J. L., Lowe, D. C., Myhre, G., Nganga, J., Prinn, R., Raga, G., Schulz, M., and Van Dorland, R.: Changes in atmospheric Cconstituents and in radiative forcing, in: Climate Change 2007: The Physical Science Basis. Contribution of Working Group I to the Fourth Assessment Report of the Intergovernmental Panel on Climate Change, edited by: Solomon, S., Qin, D., Manning, M., Chen, Z., Marquis, M., Averyt, K. B., Tignor, M., and Miller, H. L., CUP, Cambridge, UK and New York, NY, USA, 2007.

Gero, A. F. and Pitman, A. J.: The Impact of Land Cover Change on a Simulated Storm Event in the Sydney Basin, J. Appl. Meteorol. Clim., 45, 283–300, doi:10.1175/JAM2337.1, 2006.

Goldewijk, K. K.: Estimating global land use change over the past 300 years: The HYDE Database, Global Biogeochem. Cy., 15, 417–433, doi:10.1029/1999gb001232, 2001.

Hazeleger, W., Wang, X., Severijns, C., Ştefănescu, S., Bintanja, R., Sterl, A., Wyser, K., Semmler, T., Yang, S., van den Hurk, B., van Noije, T., van der Linden, E., and van der Wiel, K.: EC-Earth V2.2: description and validation of a new seamless earth system prediction model, Clim. Dynam., 1–19, doi:10.1007/s00382-011-1228-5, 2011.

IPCC: Summary for Policymakers, in: Managing the Risks of Extreme Events and Disasters to Advance Climate Change Adaptation. A Special Report of Working Groups I and II of the Intergovernmental Panel on Climate Change, edited by: Field, C. B., Barros, V., Stocker, T. F., Qin, D., Dokken, D. J., Ebi, K. L., Mastrandrea, M. D., Mach, K. J., Plattner, G.-K., Allen, S. K., Tignor, M., and Midgley, P. M., CUP, Cambridge, UK, and New York, NY, USA, 1–19, 2012.

Klein Tank, A. M. G. and Zwiers, F. W.: Guidelines on Analysis of extremes in a changing climate in support of informed decisions for adaptation World Meteorological Organization, Geneva, Switzerland, 2009.

Krinner, G., Viovy, N., de Noblet-Ducoudré, N., Ogeé, J., Polcher, J., Friedlingstein, P., Ciais, P., Sitch, S., and Prentice, I. C.: A dynamic global vegetation model for studies of the coupled atmosphere-biosphere system, Global Biogeochem. Cy., 19, GB1015, doi:10.1029/2003gb002199, 2005.

Lawrence, P. J. and Chase, T. N.: Investigating the climate impacts of global land cover change in the community climate system model, Int. J. Climatol., 30, 2066–2087, doi:10.1002/joc.2061, 2010.

Levis, S.: Modeling vegetation and land use in models of the Earth System, WIRES: Climate Change, 1, 840–856, doi:10.1002/wcc.83, 2010.

Marti, O., Braconnot, P., Dufresne, J. L., Bellier, J., Benshila, R., Bony, S., Brockmann, P., Cadule, P., Caubel, A., Codron, F., de Noblet, N., Denvil, S., Fairhead, L., Fichefet, T., Foujols, M. A., Friedlingstein, P., Goosse, H., Grandpeix, J. Y., Guilyardi, E., Hourdin, F., Idelkadi, A., Kageyama, M., Krinner, G., Lévy, C., Madec, G., Mignot, J., Musat, I., Swingedouw, D., and Talandier, C.: Key features of the IPSL ocean atmosphere model and its sensitivity to atmospheric resolution, Clim. Dynam., 34, 1–26, doi:10.1007/s00382-009-0640-6, 2010.

Niyogi, D., Pyle, P., Lei, M., Arya, S. P., Kishtawal, C. M., Shepherd, M., Chen, F., and Wolfe, B.: Urban Modification of Thunderstorms: An Observational Storm Climatology and Model Case Study for the Indianapolis Urban Region, J. Appl. Meteorol. Clim., 50, 1129–1144, doi:10.1175/2010jamc1836.1, 2011.

Pielke, R. A., Pitman, A., Niyogi, D., Mahmood, R., McAlpine, C., Hossain, F., Goldewijk, K. K., Nair, U., Betts, R., Fall, S., Reichstein, M., Kabat, P., and de Noblet, N.: Land use/land cover changes and climate: modeling analysis and observational evidence, WIRES: Climate Change, 2, 828–850, doi:10.1002/wcc.144, 2011.

Pielke Sr., R. A.: Influence of the spatial distribution of vegetation and soils on the prediction of cumulus convective rainfall, Rev. Geophys., 39, 151–177, doi:10.1029/1999rg000072, 2001.

Pitman, A. J.: The evolution of, and revolution in, land surface schemes designed for climate models, Int. J. Climatol., 23, 479–510, 2003.

Pitman, A. J., de Noblet-Ducoudré, N., Cruz, F. T., Davin, E. L., Bonan, G. B., Brovkin, V., Claussen, M., Delire, C., Ganzeveld, L., Gayler, V., van den Hurk, B. J. J. M., Lawrence, P. J., van der Molen, M. K., Müller, C., Reick, C. H., Seneviratne, S. I., Strengers,

B. J., and Voldoire, A.: Uncertainties in climate responses to past land cover change: First results from the LUCID intercomparison study, Geophys. Res. Lett., 36, L14814, doi:10.1029/2009gl039076, 2009.

Pitman, A. J., Avila, F. B., Abramowitz, G., Wang, Y. P., Phipps, S. J., and de Noblet-Ducoudre, N.: Importance of background climate in determining impact of land-cover change on regional climate, Nat. Clim. Change, 1, 472–475, 2011.

Raddatz, T., Reick, C., Knorr, W., Kattge, J., Roeckner, E., Schnur, R., Schnitzler, K. G., Wetzel, P., and Jungclaus, J.: Will the tropical land biosphere dominate the climate-carbon cycle feedback during the twenty-first century?, Clim. Dynam., 29, 565–574, doi:10.1007/s00382-007-0247-8, 2007.

Ramankutty, N. and Foley, J. A.: Estimating historical changes in global land cover: Croplands from 1700 to 1992, Global Biogeochem. Cy., 1 3, 997–1027, 1999.

Roeckner, E., Brokopf, R., Esch, M., Giorgetta, M., Hagemann, S., Kornblueh, L., Manzini, E., Schlese, U., and Schulzweida, U.: Sensitivity o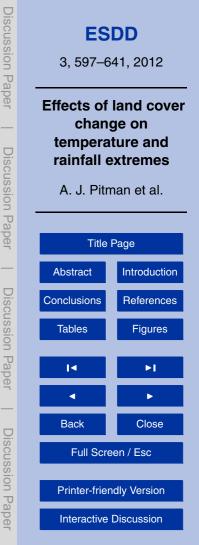f Simulated Climate to Horizontal and Vertical Resolution in the ECHAM5 Atmosphere Model, J. Climate, 19, 3771–3791, doi:10.1175/jcli3824.1, 2006.

Salas-Mélia, D., Chauvin, F., Déqué, M., Douville, H., Guérémy, J. F., Marquet, P., Planton, S., Royer, J. F., and Tyteca, S.: Description and validation of the CNRM-CM3 global coupled climate model, CNRM working note 103, http://www.cnrm.meteo.fr/scenario2004/paper_cm3.pdf (last access: 5 July 2012), 2005.

Schar, C., Luthi, D., Beyerle, U., and Heise, E.: The Soil-Precipitation Feedback: A Process Study with a Regional Climate Model, J. Climate, 12, 722–741, doi:10.1175/1520-0442(1999)012<0722:TSPFAP>2.0.CO;2, 1999.

Seneviratne, S. I., Luthi, D., Litschi, M., and Schar, C.: Land-atmosphere coupling and climate change in Europe, Nature, 443, 205–209, 2006.

Seneviratne, S. I., Corti, T., Davin, E. L., Hirschi, M., Jaeger, E. B., Lehner, I., Orlowsky, B., and Teuling, A. J.: Investigating soil moisture-climate interactions in a changing climate: A review, Earth-Sci. Rev., 99, 125–161, doi:10.1016/j.earscirev.2010.02.004, 2010.

Stefanon, M., Drobinski, P., D'Andrea, F., and de Noblet-Ducoudre, N.: Effects of interactive vegetation phenology on the 2003 summer heat waves, J. Geophys. Res., in review, 2012.

Teuling, A. J., Seneviratne, S. I., Stockli, R., Reichstein, M., Moors, E., Ciais, P., Luyssaert, S., van den Hurk, B., Ammann, C., Bernhofer, C., Dellwik, E., Gianelle, D., Gielen, B., Grunwald, T., Klumpp, K., Montagnani, L., Moureaux, C., Sottocornola, M., and Wohlfahrt, G.:

Contrasting response of European forest and grassland energy exchange to heatwaves, Nat. Geosci., 3, 722–727, 2010.

van der Molen, M. K., van den Hurk, B. J., and Hazeleger, W.: A dampened land use change climate response towards the tropics, Clim. Dynam., 37, 2035–2043, doi:10.1007/s00382-011-1018-0, 2011.

Voldoire, A.: Quantifying the impact of future land-use changes against increases in GHG concentrations, Geophys. Res. Lett., 33, L04701, doi:10.1029/2005gl024354, 2006.

Zhang, X., Alexander, L., Hegerl, G. C., Jones, P., Tank, A. K., Peterson, T. C., Trewin, B., and Zwiers, F. W.: Indices for monitoring changes in extremes based on daily temperature and precipitation data, WIRES: Climate Change, 2, 851–870, doi:10.1002/wcc.147, 2011.

Zhao, M. and Pitman, A. J.: The impact of land cover change and increasing carbon dioxide on the extreme and frequency of maximum temperature and convective precipitation, Geophys. Res. Lett., 29, 1078, doi:10.1029/2001gl013476, 2002.

Table 1. List of climate models and associated Land-Surface Models used in the first LUCID set of experiments.

Climate model	Reference	Spatial resolution	Land-surface model	Reference
ARPEGE	Salas-Mélia et al. (2005)	$2.8° \times 2.8°$	ISBA	Voldoire (2006)
ECHAM5	Roeckner et al. (2006)	$3.75° \times 3.75°$	JSBACH	Raddatz et al. (2007)
ECEarth	www.ecmwf.int/research/ifsdocs/CY31r1/	$1.8° \times 1.8°$	HTESSEL	Hazeleger et al. (2011)
IPSL	Marti et al. (2010)	$2.5° \times 3.75°$	ORCHIDEE	Krinner et al. (2005)

Table 2. Description of simulations performed by each climate model.

Experiment name	Description of the experiment	CO$_2$ (ppm)	Year of vegetation map	SSTs
PI	Pre-industrial Simulation, with CO$_2$, greenhouse gases, aerosols, land-cover map and SSTs being prescribed at their pre-industrial values	280	1870	Prescribed 1870–1900
PD	Present-day Simulation, with present-day CO$_2$, land-cover map, SSTs and sea-ice extent. Other greenhouse gases have been added to the CO$_2$ concentration as CO$_2$-equivalent[*], while aerosols have been kept to their pre-industrial values.	375	1992	Prescribed 1972–2002
PIv	Pre-industrial Simulation with CO$_2$, greenhouse gases, aerosols and SSTs being prescribed at their pre-industrial value, but with present-day land-cover map	280	1992	Prescribed 1870–1900
PDv	Present-day Simulation, with present-day CO$_2$, SSTs and sea-ice extent. Other greenhouse gases have been added to the CO$_2$ concentration as CO$_2$-equivalent, while aerosols have been kept to their pre-industrial values. But land-cover map is pre-industrial.	375	1870	Prescribed 1972–2002

[*] Except in EC-EARTH where those were changed proportionally to CO$_2$ changes.

Table 3. A selection of the temperature indices recommended by the ETCCDI and used in this study (definitions can be found at http://cccma.seos.uvic.ca/ETCCDI/list_27_indices.shtml). Note that ETCCDI expresses the temperature frequency indices (TX10p, TN10p, TX90p and TN90p) in percentages, but the scale used here is in number of days per 3-month season (DJF, MAM, JJA, SON). Differences in the percentile-based indices (including WSDI and CSDI) relate to the 10th and 90th percentiles of simulation PI.

Index	Definition		Unit
	(A) Temperature		
	Intensity		
TXn	Min T_{max}	Coldest seasonal daily maximum temperature	˚C
TNn	Min T_{min}	Coldest seasonal daily minimum temperature	˚C
TXx	Max T_{max}	Warmest seasonal daily maximum temperature	˚C
TNx	Max T_{min}	Warmest seasonal daily minimum temperature	˚C
	Duration		
CSDI	Cold spell duration indicator	Annual number of days with at least 6 consecutive days when $T_{min} <$ 10th percentile	Days per year
WSDI	Warm spell duration indicator	Annual number of days with at least 6 consecutive days when $T_{max} >$ 90th percentile	Days per year
	Frequency		
TX10p	Cool days	Number of days when $T_{max} <$ 10th percentile	Days per season
TN10p	Cool nights	Number of days when $T_{min} <$ 10th percentile	Days per season
TX90p	Warm days	Number of days when $T_{max} >$ 90th percentile	Days per season
TN90p	Warm nights	Number of days when $T_{min} >$ 90th percentile	Days per season
	(B) Rainfall		
RX1day		Maximum daily rainfall	mm
RX5day		Maximum rainfall occurring over a 5 day consecutive period	mm

Table 4. Correlation coefficients between the change in precipitation and the change in RX5day due to LULCC and between the change in RX5day and the change in the sum of the latent and sensible heat fluxes.

	Correlation					
	ΔP versus ΔRX5day			ΔRX5day versus ΔQ_t		
Model	Eurasia	North America	S. E. Asia	Eurasia	North America	S. E. Asia
ECEarth	0.73	0.72	0.75	0.35	0.30	0.42
IPSL	0.02	0.00	0.02	0.03	0.03	0.03
ECHAM5	0.00	0.01	0.00	0.00	0.02	0.00
ARPEGE	0.20	0.24	0.26	0.19	0.13	0.13

Table 5. Caption on next page.

| | MAM | | | | | | | | | | |
| | dLULCC @ 280 | | | | dLULCC @ 375 | | | | dCO2 (1870) | | | |
	N. Hemisphere	North America	Eurasia	S.E. Asia	N. Hemisphere	North America	Eurasia	S.E. Asia	N. Hemisphere	North America	Eurasia	S.E. Asia
ARPEGE												
TXx	9	16	12	6	9	16	14	-	49	29	51	46
TNx	18	40	25	11	16	33	25	14	64	68	60	69
TXn	16	40	36	-	11	34	29	-	36	12	63	15
TNn	23	45	46	18	20	48	33	13	52	41	69	40
TN10p	33	58	50	38	25	59	37	22	87	96	94	85
TX10p	29	51	45	19	19	47	41	13	69	88	94	35
TN90p	29	49	48	14	25	52	52	13	87	97	98	99
TX90p	30	62	53	8	23	53	49	-	71	78	83	54
DTR	23	44	26	21	19	36	33	13	39	8	46	61
RX1day	12	10	16	-	-	-	-	-	14	12	8	26
RX5day	13	15	19	7	-	5	-	-	15	11	10	28
ECHAM5												
TXx	8	23	-	13	7	22	10	8	58	51	47	61
TNx	8	16	13	10	-	16	-	-	67	64	53	85
TXn	-	-	-	-	-	10	9	-	41	44	8	44
TNn	-	5	-	13	-	11	-	-	58	56	26	68
TN10p	-	-	10	10	6	34	-	10	93	95	80	92
TX10p	6	11	9	-	10	40	-	10	81	82	71	61
TN90p	6	8	8	11	-	11	7	-	87	90	90	100
TX90p	7	16	10	13	8	10	13	6	76	55	78	82
DTR	8	16	11	21	11	12	10	11	35	18	25	22
RX1day	-	-	7	6	6	7	10	7	13	-	8	21
RX5day	6	-	9	7	5	-	9	7	12	8	6	25
ECEarth												
TXx	13	40	14	-	17	51	37	8	25	18	20	33
TNx	11	27	15	-	15	36	37	6	38	40	42	46
TXn	10	18	17	-	-	8	8	-	21	12	19	17
TNn	12	21	21	-	7	12	15	7	38	26	26	35
TN10p	23	37	36	15	16	34	37	13	75	74	78	76
TX10p	19	36	20	7	11	41	20	-	46	45	58	44
TN90p	18	37	23	15	16	34	35	8	64	52	72	86
TX90p	23	62	30	13	18	52	37	7	37	19	38	47
DTR	10	27	10	-	11	33	17	6	30	14	12	18
RX1day	-	10	-	-	-	5	-	-	9	5	-	10
RX5day	-	8	-	-	-	5	-	-	8	-	-	7
IPSL												
TXx	11	26	32	7	14	32	29	8	49	48	23	60
TNx	9	7	17	14	9	25	9	15	56	56	38	79
TXn	8	10	21	-	11	25	19	-	31	19	14	38
TNn	8	8	10	6	9	23	12	-	39	33	20	57
TN10p	12	5	24	21	9	18	15	7	76	90	54	90
TX10p	13	25	36	7	12	30	24	8	73	88	51	82
TN90p	11	12	6	19	13	29	10	14	69	79	60	97
TX90p	14	40	17	7	17	42	21	13	62	56	47	86
DTR	18	48	17	21	18	33	23	21	43	12	23	39
RX1day	-	-	-	6	6	5	6	8	16	5	6	17
RX5day	-	7	-	7	5	5	6	7	17	7	10	17

| 5 | 20 | 40 | 60 | 80 | 90 | 95 |

Percent of significant grid points

Title Page

Abstract | Introduction

Conclusions | References

Tables | Figures

◀◀ | ▶▶

◀ | ▶

Back | Close

Full Screen / Esc
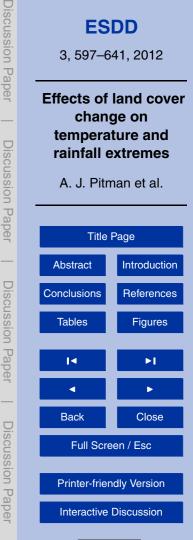
Printer-friendly Version

Interactive Discussion

Table 5. Percent of significant grid points in four regions for MAM and JJA for each model used in this paper. The first set of columns of data is for the impact of LULCC at 280 ppmv, the second set of columns is for the impact of LULCC at 375 ppmv. The final set of columns is for the impact of the increase in CO_2 from 280 ppmv to 375 ppmv. Dashes represent points where no grid points were significant.

	JJA											
	dLULCC @ 280				dLULCC @ 375				dCO2 (1870)			
	N. Hemisphere	N. America	Eurasia	S.E. Asia	N. Hemisphere	N. America	Eurasia	S.E. Asia	N. Hemisphere	N. America	Eurasia	S.E. Asia
ARPEGE												
TXx	18	45	26	10	17	36	35	14	71	93	75	46
TNx	23	52	37	13	21	52	44	13	88	99	79	96
TXn	6	15	10	-	7	5	16	-	56	53	52	58
TNn	24	52	42	13	22	48	32	21	73	89	58	71
TN10p	37	82	57	26	30	71	51	26	94	100	90	99
TX10p	12	34	15	-	14	26	28	6	77	93	71	64
TN90p	30	63	48	18	31	68	53	29	96	100	96	100
TX90p	21	44	32	15	20	44	37	22	82	99	86	67
DTR	23	48	39	17	29	53	46	29	35	19	38	36
RX1day	6	14	11	-	8	14	7	11	21	16	21	26
RX5day	9	21	13	6	8	12	7	11	21	12	21	22
ECHAM5												
TXx	12	44	16	11	8	33	7	14	89	73	91	83
TNx	7	27	10	-	6	25	-	8	97	85	100	96
TXn	5	23	-	-	7	27	-	-	86	70	85	86
TNn	-	7	-	-	-	14	-	-	96	96	99	100
TN10p	9	44	9	7	8	34	-	10	99	95	100	100
TX10p	11	52	13	-	11	51	9	10	95	79	100	92
TN90p	10	27	19	-	8	36	6	10	99	95	100	100
TX90p	13	42	19	8	9	48	7	15	96	78	100	100
DTR	14	47	24	8	14	60	14	18	34	51	25	11
RX1day	5	11	10	-	8	21	11	8	24	25	15	42
RX5day	6	27	8	-	8	22	10	7	24	32	17	44
ECEarth												
TXx	25	52	43	6	18	64	25	7	42	52	29	36
TNx	21	40	40	-	16	48	27	-	58	73	40	81
TXn	6	14	-	-	10	53	-	6	39	47	37	38
TNn	12	22	24	-	14	45	30	7	63	59	63	63
TN10p	24	42	40	11	21	62	39	11	90	93	83	90
TX10p	15	37	19	-	17	60	23	6	60	74	58	79
TN90p	23	48	44	6	23	59	34	7	82	89	60	99
TX90p	26	62	44	10	24	68	30	6	61	78	42	76
DTR	16	42	25	6	18	67	20	7	24	19	17	18
RX1day	5	10	6	6	6	15	-	6	8	14	-	17
RX5day	6	5	7	-	7	14	8	7	8	11	-	13
IPSL												
TXx	16	5	26	21	11	18	25	11	77	53	57	92
TNx	20	21	33	14	14	33	23	13	89	62	88	97
TXn	-	21	-	7	-	5	-	-	71	70	71	60
TNn	5	8	-	-	6	14	9	-	75	71	75	83
TN10p	12	22	15	13	11	29	11	17	97	88	100	100
TX10p	11	21	17	15	8	12	11	18	96	88	98	93
TN90p	23	29	28	18	17	41	22	19	95	84	97	100
TX90p	19	7	35	28	14	19	27	13	90	71	75	97
DTR	20	33	19	26	21	40	18	38	41	36	40	42
RX1day	8	-	16	13	7	14	16	10	14	7	8	14
RX5day	9	7	18	8	9	15	20	14	17	11	8	18

5	20	40	60	80	90	95

Percent of significant grid points

Discussion Paper | Discussion Paper | Discussion Paper | Discussion Paper

Title Page

Abstract | Introduction

Conclusions | References

Tables | Figures

|◀ | ▶|

◀ | ▶

Back | Close

Full Screen / Esc
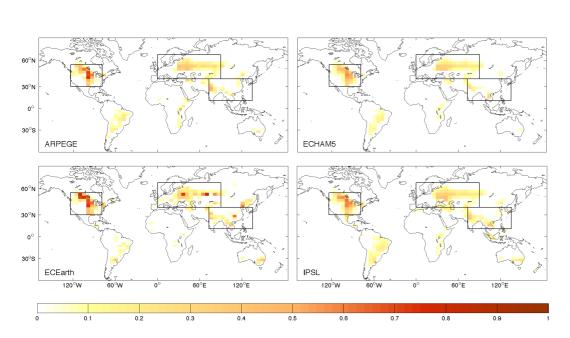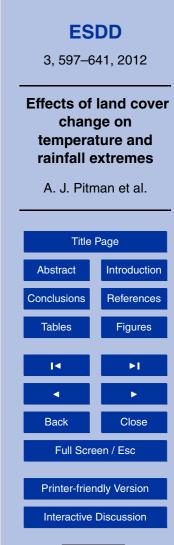
Printer-friendly Version

Interactive Discussion

Fig. 1. Fraction of vegetation cover converted from natural vegetation to cropland for the four models. The boxes on each panel outline the regions of intense LULCC used for the scatter plots (North America, 30–55° N, 78–123° W; Eurasia, 40–65° N, 0–90° E; and South East Asia, 11–40° N, 73–135° E).
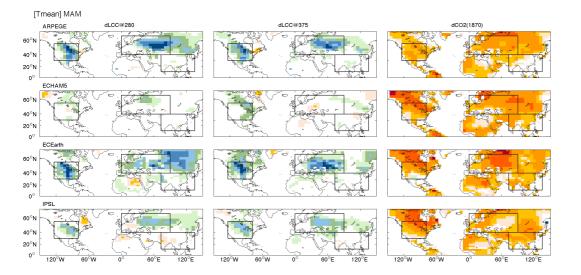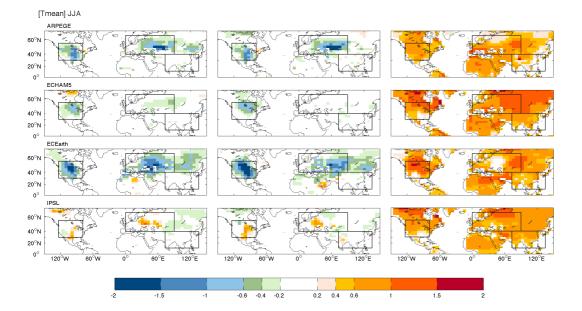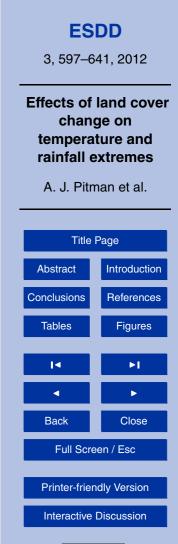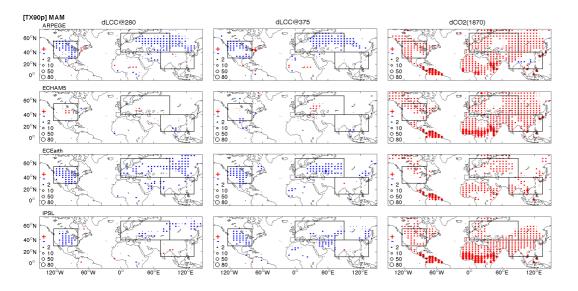
Fig. 2. Caption on next page.

Full Screen / Esc

Fig. 2. Change in the mean surface air temperature (°C) in March-April-May (MAM) and June-July-August (MAM) for the four models. The left column is the impact on the mean surface air temperature of LULCC at a CO_2 concentration of 280 ppmv (PIv-PI). The middle column is the impact of LULCC at a CO_2 concentration of 375 ppmv (PD-PDv). The right column shows the impact of the increase in CO_2 alone using land cover reflecting 1870 conditions (PDv-PI).

Fig. 3. Caption on next page.

Fig. 3. As Fig. 2 but for mean precipitation (mm day^{-1}).

Fig. 4. Caption on next page.

Title Page

Abstract | Introduction

Conclusions | References

Tables | Figures

◀ | ▶|

◀ | ▶

Back | Close

Full Screen / Esc

Printer-friendly Version

Interactive Discussion

Fig. 4. As Fig. 2 but for the warmest seasonal daily maximum temperature (TXx, ˚C). Only the grid points that are statistically significant at the 95 % level using the two-tailed Kolmogorov-Smirnov test are shown (red for warming and blue for cooling). The magnitude of the change is indicated by the size of the circles.

Fig. 5. Caption on next page.

Fig. 5. As Fig. 4 but for the coldest seasonal daily minimum temperature (TNn, °C).

Fig. 6. Caption on next page.

Fig. 6. As Fig. 4 but for the number of days when $T_{max} > 90$th percentile relative to the PI simulation (TX90p, days/season).

Fig. 7. As Fig. 4 but for the warm spell duration index (WDSI, days/year).

Fig. 8. As Fig. 4 but for the cold spell duration index (CSDI, days/year). Note that for this index, blue indicates an increase in the number of cold days and red indicates an decrease in the number of cold days.

Fig. 9. Caption on next page.

Title Page

Abstract | Introduction

Conclusions | References

Tables | Figures

◄ | ►

Back | Close

Full Screen / Esc

Printer-friendly Version

Interactive Discussion
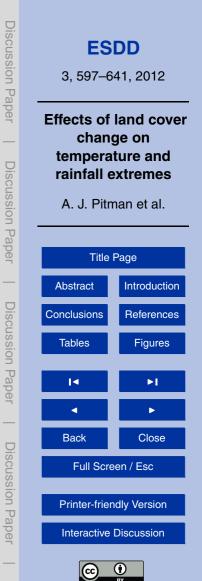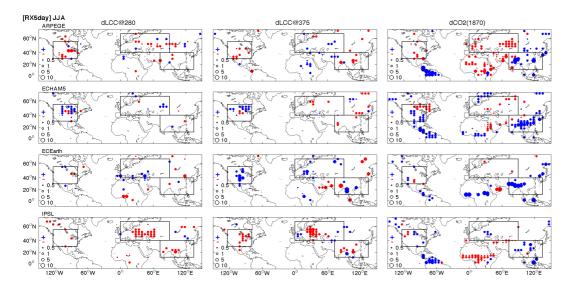
Fig. 9. As Fig. 4 but for the maximum rainfall occurring over a 5 day consecutive period (RX5day, mm). Note that for this index, blue indicates increased rainfall and red indicates decreased rainfall.